Physics of Plasmas ACCEPTED MANUSCRIPT

AIP Publishing

This is the author's peer reviewed, accepted manuscript. However, the online version of record will be different from this version once it has been copyedited and typeset.

PLEASE CITE THIS ARTICLE AS DOI: 10.1063/5.0094038

# Dispersion relation for the dust ionization and dust acoustic waves in the gas discharge complex plasma

D. I. Zhukhovitskii[1, a)]
*Joint Institute of High Temperatures, Russian Academy of Sciences, Izhorskaya 13, Bd. 2, 125412 Moscow, Russia*

(Dated: 12 May 2022)

A theoretical approach is developed for the dust ionization and dust acoustic waves propagating in the cloud of microparticles in the low-pressure gas discharge under microgravity conditions. The theory explores the fluid approximation for the microparticle subsystem of complex plasma combined with the kinetic equation for the ions. In the one-dimensional approximation, the wave equation is obtained, whose solution defines the dispersion relation for the waves in complex plasma involving the oscillations of microparticles. Obtained dispersion relation unifies both the dust ionization and the dust acoustic waves (DIW and DAW, respectively). According to this dispersion relation, the effect of microparticles on the recombination rate leads to a number of peculiarities. Among them, existence of the minimum frequency, above which the wave propagation is possible, a weak dependence of the DIW wave number on the frequency, and a high phase velocity of DIW as compared to DAW. It is demonstrated that no instability of DIW is possible whereas DAW can reveal instability under proper conditions. Calculation results correlate with those obtained in a recent experiment.

PACS numbers: 52.27.Lw, 94.20.wf, 52.35.Fp
Keywords: dust ionization waves, dust acoustic waves, dispersion relation, microgravity, complex plasmas

## I. INTRODUCTION

Low-temperature plasmas containing from submicron to hundred micron microparticles is conventionally called the complex plasma. Various realizations of complex plasmas can be encountered in laboratory setups and technological applications.[1] In astrophysics, complex plasma can be found in the vicinity of space bodies, in comets, protoplanetary discs, planetary rings, in ionospheric and magnetospheric plasma of the planets, interplanetary and interstellar clouds, etc.[2,3] Naturally in astrophysical occurrences, the particles may not be small. Due to a significant electric charge collected on the microparticles (positive or negative), they can form extended clouds with ordered structures analogous to the liquid or solid.[4–6] These structures (microparticle clouds) can be fairly homogeneous under microgravity conditions that can be attained for long periods of time on board the International International Space Station (ISS).[7–11]

A permanent interest to the collective phenomena occurring in complex plasmas extends to the wave phenomena. Since the microparticles accumulate a considerable charge and their extended surface provides a dominating mechanism of the electron–ion recombination, they can change the plasma dynamic properties considerably even if they are not directly involved in the oscillations. Otherwise, oscillations of the microparticles proper are the key ones for the wave mode formation. Since the microparticles are massive as compared to the ions, such modes imply low wave frequencies that typically do not exceed 100 Hz. The dust acoustic waves (DAW) is this kind of wave mode, which is characterized by the proportionality dispersion relation. DAW was treated in the pioneer theoretical study[12] and then in Ref. 13 (see also Ref. 14). Predicted theoretically, DAW were then discovered in the experimental studies.[15–17] In further works, the effect of strong Coulomb coupling of the microparticles on the dispersion relation was investigated.[18–21] Nonlinear DAW are an object of recent investigations.[22,23] Among other types of investigated wave modes, the self-exciting nonlinear dust-density waves,[24] the dust ion-acoustic waves not involving the oscillation of microparticles,[25,26] dust cyclotron and drift modes[27,28] are to be mentioned.

Numerous experiments, in which both the externally excited and the self-excited DAW were observed, have been performed on the PK-4[29] facility under microgravity conditions on board the ISS. Recently, discovery of a new dust wave mode named the dust ionization wave (DIW) on this facility was reported.[30] In this experiment, the microparticles were injected in the DC polarity-switching low-pressure argon or neon discharge. These particles formed a cloud elongated in the direction of the discharge tube axis. The DIW progressing waves were externally excited in this cloud by the oscillating field of a special electrode. The DIW phase velocity proved to be very high as compared to the DAW velocity, and the wave number was found almost independent of the frequency. Since the DIW frequency did not exceed 20 Hz, the observed DIW mode obviously implied the microparticle oscillations, in contrast to the conventional ionization waves in a pure gas without microparticles.[31] Additionally, it was found that DIW propagation seemed to be impossible below some frequency limit on the order of several Hz.

Theoretical analysis in Ref. 30 was restricted to formulation of the master equations based on the fluid approximation and solely the simplest order-of-magnitude estimations were derived for the characteristic DIW quantities. Objective of this work is to demonstrate that DIW and DAW are in fact the long- and short-wave extremes of oscillations involving the microparticles. To this end, an accurate solution

---

[a)] Electronic mail: dmr@ihed.ras.ru.

Physics of Plasmas ACCEPTED MANUSCRIPT

This is the author's peer reviewed, accepted manuscript. However, the online version of record will be different from this version once it has been copyedited and typeset.

PLEASE CITE THIS ARTICLE AS DOI: 10.1063/5.0094038

AIP Publishing

of the master equations is found in the linear approximation. Here, in the momentum equation, we now take into account the proper compressibility of the microparticle cloud responsible for DAW, friction of the microparticles against the neutrals that leads to wave damping, and the interaction between the streaming ions and the microparticles leading to DAW instability. The equation set is reduced to a single wave equation for the electron number density whose solution defines a unified dispersion relation for both DIW and DAW. Both modes merge at the minimum frequency of wave propagation. It is demonstrated that DIW is a long-wave mode where the wave number is almost independent of the frequency while DAW is a short-wave branch. Performed analysis shows that DIW emerge if a spatial perturbation of the microparticle number density can give rise to a perturbation of the rate of recombination under the conditions when the recombination on the microparticle surface dominates. Therefore, perturbation of the recombination rate causes the charge separation that is the source of the wave electric field. Analysis of the imaginary part of frequency in the dispersion relation makes it possible to conclude that no instability of DIW that could result in their self-excitation is possible. At the same time, their damping length is long enough due to a high DIW phase velocity. In contrast, the DAW damping length is typically very short, which complicates their external excitation. However, they can reveal instability under proper conditions resulting in their self-excitation. Thus, the theoretical approach to a unified theory of DIW and DAW that correlates with available experimental data is proposed.

The paper is organized as follows. In Sec. II, the master equations of the fluid approximation are formulated, and the assumptions involved in these equations are discussed. The master equations are linearized and solved in Sec. III, where the dispersion relation is derived, and the phase and group velocities are calculated. Peculiarities of DIW and DAW modes are analyzed and compared in Sec. IV. Section V is devoted to application of the obtained analytical results for simulation of DIW under the experimental conditions[30] and to the discussion of some inconsistency between the theory and experiment. The results of this study are summarized in Sec. VI.

## II. MASTER EQUATIONS

The theory discussed in this Section implies typical parameters of the experiment.[30] For the sake of simplicity, we will consider idealized conditions when a plane wave propagates in the infinite weakly inhomogeneous microparticle cloud in the polarity-switching DC low-pressure gas discharge. For the microparticle cloud, we explore the one-dimensional fluid approximation. The polarity switching frequency of 500 Hz[30] is so high for the relatively massive microparticles that their oscillations are not observable. This allows one to introduce a principle simplification for the analyses of a complex system realized in experiment implying averaging of all plasma parameters over the period of polarity switching. Apparently, such averaging is possible for sufficiently small perturbations introduced by DIW in the weakly inhomogeneous complex plasma.

The implied parameters of complex plasma are such that the recombination on the particle surface dominates over that on the tube walls so the latter can be ignored. Under such conditions, each hump in the microparticle number density distribution leads to the increase in the recombination rate and, consequently, to a local drop in the electron and ion number densities. On the contrary, a hollow of the microparticle number density results in a local increase of the electron and ion number densities. Thus, an electric field occurs in the complex plasma due to the charge separation. This electric field averaged over the polarity switching period drives the microparticle oscillations.

Since both DIW and DAW branches imply the microparticle oscillations, we intend to unify their treatment in a single formalism. With this in mind, we will complete the momentum equation by the corresponding terms. First, we include the term due to the microparticle pressure gradient. Assuming that the DAW velocity is constant one can introduce the DAW velocity phenomenologically. We also take into account the DAW instability that can arise from the interaction between the microparticles and streaming ions and lead to the self-excited oscillations. Different mechanisms of the instability development are to be found in the literature (e.g., Refs. 32–34). As an example, we borrow the mechanism discussed in Ref. 34 and based on the ionization equation of state (IEOS) model[35] according to which the balance between the ambipolar electric field driving force and the ion drag force becomes unstable if inhomogeneity of the microparticle cloud exceeds some threshold.

According to IEOS gradients of the electron and ion number densities are related to the gradient of the number density of microparticles that defines the instability development threshold. Indeed, in the experiment the microparticle distribution along the discharge tube axis is inhomogeneous.[30] At the same time, the complex plasma inhomogeneity implies existence of the zero-order ambipolar electric field, which is small along with the density gradients of the charged species. This zero-order electric field drives the ion flow.

In the low-pressure radio frequency gas discharge under microgravity conditions, the microparticles are exposed to the force from the ambipolar electric field $\mathbf{E}$ and to the ion drag force. The total force $\mathbf{f}$ acting on unit volume of the microparticle cloud is[35]

$$\mathbf{f} = \left[\frac{3}{8}\left(\frac{4\pi n_d}{3}\right)^{1/3} \lambda e n_i - Z e n_d\right]\mathbf{E}, \tag{1}$$

where $n_d$ and $n_i$ are the number density of the microparticles and ions, respectively; $\lambda = \lambda_a(1+3/8\rho)^{-1}$ is the total ion mean free path including the ion–particle collisions, $\lambda_a$ is the ion mean free path with respect to the collisions with atoms, $\rho = (3/4\pi n_{d0})^{1/3}\lambda_a^{-1}$; $e$ is the elementary electric charge; $Z$ is the particle charge in units of the electron charge $-e$. In what follows, we will denote the stationary state quantities by subscript 0, and their perturbations, by prime, so that $n_{e,i,d} = n_{e,i,d0} + n'_{e,i,d}$ for the number density of electrons, ions, and microparticles, respectively. The stationary state described by

Physics of Plasmas
ACCEPTED MANUSCRIPT
This is the author's peer reviewed, accepted manuscript. However, the online version of record will be different from this version once it has been copyedited and typeset.
PLEASE CITE THIS ARTICLE AS DOI: 10.1063/5.0094038
AIP Publishing

IEOS is maintained by vanishing the force (1),

$$Zn_{d0} = \frac{3}{8}\left(\frac{4\pi n_{d0}}{3}\right)^{1/3}\lambda n_{i0}. \tag{2}$$

If we apply the equation for the stationary microparticle charge, the overall quasineutrality condition for the complex plasma, and fix a relation between the small perturbations $n'_e$, $n'_i$, and $n'_d$ then the total force acting on a unit mass can be written as $An'_d/n_{d0}$, where the coefficient $A$ depends on the assumed relation between the perturbations.[34] For example, for $n'_e = \mathrm{const}$ (typical for DAW, see Sec. V),

$$A = \frac{2}{9}\frac{ZT_e(2-3\gamma)}{M}\frac{d\ln n_{d0}}{dx}. \tag{3}$$

where

$$\gamma = 1 - 2.8\frac{a\tau^{5/2}}{\lambda_a}\left(\frac{m_e}{m_i}\right)^{1/2}\Phi^3 e^{\Phi}, \tag{4}$$

$T_e$ is the electron temperature, $M$ is the microparticle mass, $x$ is the coordinate, $a$ is the microparticle radius, $\tau = T_e/T_i$, $T_i$ is the ion temperature, $m_e$ and $m_i$ are the electron and ion mass, respectively, and $\Phi = Ze^2/aT_e$ is the dimensionless microparticle potential. As is seen from Eq. (3), the instability development is defined by the microparticle cloud inhomogeneity $dn_{d0}/dx$. For the case $n'_e = n'_i$ characteristic of DIW, the factor $A$ differs from (3) by a numerical factor on the order of unity. Since our purpose is to demonstrate that self-excitation of DIW is impossible, we will neglect this difference.

Additionally, friction of the microparticles against neutrals should be taken into account irrespective of the wave mode. Thus, the complete momentum equation, where all quantities are functions of the coordinate $x$ and time $t$ is written as

$$\frac{\partial u}{\partial t} + u\frac{\partial u}{\partial x} = -\frac{c_a^2}{n_d}\frac{\partial n_d}{\partial x} + \frac{Ze}{M}\frac{\partial \varphi}{\partial x} - \nu u + A\frac{n'_d}{n_{d0}}, \tag{5}$$

where $u$ is the particle velocity field; $c_a$ is the DAW velocity; $\varphi$ is the wave electric field potential; $\nu = (8\sqrt{2\pi}/3)\delta m_a n_a v_{T_a} a^2/M$ is the inverse time of particle deceleration in a gas (friction coefficient),[36] $\delta \simeq 1.4$ is the accommodation coefficient; $m_a$ is the mass of a gas molecule; $n_a$ and $v_{T_a} = (T_a/m_a)^{1/2}$ are the number density and thermal velocity of the neutrals, respectively, and $T_a = 300$ K is the gas temperature. In what follows, we will neglect the dependence of $Z$ on the complex plasma parameters. The condition that stipulates constancy of $Z$ will be discussed below. It is worth mentioning that due to high electron mobility, the microparticles acquire a considerable negative charge.

In Eq. (5), solely the second term on the right-hand side corresponds to the DIW mode and it will be shown in Sec. IV that the first and the last terms can be neglected in this mode. Instead, the second term is negligibly small in the DAW mode, for which the first and the last two terms are the key ones. The third term responsible for friction cannot be disregarded for both modes. Hence, (5) is in fact a simple extrapolation between the DIW and DAW extremes.

Remaining master equations include the microparticles balance equation

$$\frac{\partial n_d}{\partial t} + \frac{\partial}{\partial x}(un_d) = 0 \tag{6}$$

and the equation for electrons. Due to the high mobility of electrons, their distribution is close to the equilibrium one corresponding to the electron temperature $T_e$. We adopt the approximation of the Boltzmann distribution for the electrons, which is commonly used for the low-pressure gas discharge,

$$\frac{\partial \varphi}{\partial x} = \frac{T_e}{en_e}\frac{\partial n_e}{\partial x}. \tag{7}$$

Since the ions in the low-pressure gas discharge are strongly nonequilibrium, their treatment is based on the balance equation

$$\frac{\partial n_i}{\partial t} + \frac{\partial J}{\partial x} = Q, \tag{8}$$

where $J$ is the ion flux, and $Q$ is the total number of ions produced in unit volume per unit time. Since the ion relaxation time is typically much smaller than both the discharge polarity switching time and the inverse wave frequency due to the small ion mass, this equation can be treated in the stationary approximation, i.e., we set $\partial n_i/\partial t = 0$. The ion flux is a sum of the drift and diffusion components,

$$J = -Dn_i\frac{T_e}{T_i}\frac{\partial \ln n_e}{\partial x} - D\frac{\partial n_i}{\partial x}, \tag{9}$$

where $D$ is the coefficient of ion diffusion in the gas of neutrals, and for the first term on the right-hand side, we used the Einstein–Smoluchowski equation for the ion drift in the electric field whose magnitude $-\partial\varphi/\partial x$ is defined by Eq. (7). If we assume the ionization by electron impact and the recombination of ions on the microparticle surface to be the dominating mechanisms contributing to $Q$ then

$$Q = Kn_e n_a - Rn_i n_d, \tag{10}$$

where $K$ is the coefficient of ionization by electron impact and $R$ is the coefficient of recombination on the microparticle surface. Note that $K$ is an effective quantity defined by the stationary number densities of electrons $n_{e0}$ and ions $n_{i0}$ rather that a true one because a real ionization process in argon or neon involves intermediate excited states. Thus, within the above-formulated approximation the ion balance equation is written as

$$\frac{\partial}{\partial x}\left(D\frac{T_e}{T_i}\frac{n_i}{n_e}\frac{\partial n_e}{\partial x} + D\frac{\partial n_i}{\partial x}\right) = Rn_i n_d - Kn_e n_a. \tag{11}$$

Note that Eq. (11) does not require $n_e = n_i$. From (10), the stationary ionization–recombination balance condition is

$$Rn_{d0}n_{i0} = Kn_a n_{e0}. \tag{12}$$

In what follows, in contrast to Ref. 30, no special limitation will be imposed on the variations of the number densities of

Physics of Plasmas ACCEPTED MANUSCRIPT

This is the author's peer reviewed, accepted manuscript. However, the online version of record will be different from this version once it has been copyedited and typeset.

PLEASE CITE THIS ARTICLE AS DOI: 10.1063/5.0094038

electrons or ions. Therefore, the set of master equations must be completed by the Poisson equation

$$\frac{\partial^2 \varphi}{\partial x^2} = 4\pi e(Zn_d + n_e - n_i). \tag{13}$$

In Sec. III, the linearized equations (5)–(7), (11)–(13) will be reduced to a single wave equation whose solution defines the unified dispersion relation for DIW and DAW modes.

## III. UNIFIED DISPERSION RELATION

With due regard for the linearized Eq. (7),

$$\frac{\partial \varphi}{\partial x} = \frac{T_e}{en_{e0}} \frac{\partial n'_e}{\partial x}, \tag{14}$$

linearization of (5) and of (6) yields

$$\begin{gathered}\frac{\partial u}{\partial t} = -\frac{c_a^2}{n_{d0}} \frac{\partial n'_d}{\partial x} + \frac{Zv_d^2}{n_{e0}} \frac{\partial n'_e}{\partial x} - \nu u + A\frac{n'_d}{n_{d0}},\\ \frac{\partial n'_d}{\partial t} + n_{d0}\frac{\partial u}{\partial x} = 0,\end{gathered} \tag{15}$$

where $v_d^2 = T_e/M$. It follows from linearized Eq. (13) and Eq. (14) that

$$\frac{\partial^2 n'_e}{\partial x^2} = r_{De}^{-2}(Zn'_d + n'_e - n'_i), \tag{16}$$

where $r_{De}^2 = T_e/4\pi n_{e0}e^2$. Therefore, in the typical case $r_{De}k_d \ll 1$, where $k_d$ is the characteristic wave number, Eq. (16) is degenerated to the quasineutrality equation

$$Zn'_d + n'_e = n'_i. \tag{17}$$

The latter equation makes it possible to linearize Eq. (11) as

$$D\frac{T_e}{T_i}\frac{n_{i0}}{n_{e0}}\frac{\partial^2 n'_e}{\partial x^2} = \frac{Kn_a}{1+H}\left[\left(2+\frac{1}{H}\right)Zn'_d - Hn'_e\right], \tag{18}$$

where $H = Zn_{d0}/n_{e0}$ is the Havnes parameter.

We differentiate the first Eq. (15) with respect to $x$ and substitute $\partial u/\partial x$ from the second Eq. (15) to exclude the velocity:

$$\frac{\partial^2 n'_d}{\partial t^2} - c_a^2\frac{\partial^2 n'_d}{\partial x^2} + Hv_d^2\frac{\partial^2 n'_e}{\partial x^2} + \nu\frac{\partial n'_d}{\partial t} + A\frac{\partial n'_d}{\partial x} = 0. \tag{19}$$

Then we exclude $n'_d$ from (19) using (18) to arrive at the wave equation

$$\begin{gathered}k_d^2\frac{\partial^2 n'_e}{\partial t^2} + \left(\omega_d^2 - \omega_a^2\right)\frac{\partial^2 n'_e}{\partial x^2} + \frac{\partial^4 n'_e}{\partial t^2 \partial x^2} + \nu k_d^2\frac{\partial n'_e}{\partial t}\\ +\nu\frac{\partial^3 n'_e}{\partial t \partial x^2} + Ak_d^2\frac{\partial n'_e}{\partial x} + A\frac{\partial^3 n'_e}{\partial x^3} - c_a^2\frac{\partial^4 n'_e}{\partial x^4} = 0,\end{gathered} \tag{20}$$

where

$$k_d^2 = \frac{H}{1+H}\frac{T_i}{T_e}\frac{Rn_{d0}}{D}, \tag{21}$$

$$\omega_d^2 = Zv_d^2\frac{1+2H}{1+H}\frac{T_i}{T_e}\frac{Rn_{d0}}{D}, \tag{22}$$

and $\omega_a = c_a k_d$. Note that Eqs. (21) and (22) were obtained using (12) and the relation $n_{i0}/n_{e0} = 1 + H$ following from the stationary quasineutrality condition. Obviously, $k_d$ and $\omega_d$ are the inverse length and time scale characteristics of DIW. Based on these scales, one can define a characteristic DIW velocity scale $c_d = \omega_d/k_d$. It follows from (21) and (22) that

$$c_d^2 = Zv_d^2\frac{1+2H}{H}. \tag{23}$$

Note that the equation set (5)–(7), (11)–(13) is solved rigorously (in the linear approximation) without the assumptions $n'_i = 0$ and $H \ll 1$ adopted in the previous work. This has an effect on the analytical expressions for $k_d$, $\omega_d$, and $c_d$, which are essentially different from those obtained in Ref. 30.

Equation (20) has the monochromatic plane wave solution $n'_e \sim e^{i(\omega t - kx)}$ provided that the following dispersion relation is satisfied:

$$\tilde{\omega}^2 - i2\tilde{\nu}\tilde{\omega} - q^2 + i2\beta\tilde{k} = 0, \tag{24}$$

where

$$q^2 = \alpha^2\tilde{k}^2 + 1 + \frac{1}{\tilde{k}^2 - 1}, \tag{25}$$

$\tilde{\omega} = \omega/\omega_d$, $\tilde{k} = k/k_d$, $\alpha = \omega_a/\omega_d = c_a/c_d$, $\tilde{\nu} = \nu/2\omega_d$, and the instability coefficient $\beta = A/2c_d\omega_d$ are the dimensionless quantities.

From Eq. (24), the dependence $\tilde{\omega}(\tilde{k})$ can be explicitly written in the form

$$\tilde{\omega}(\tilde{k}) = \sqrt{q^2 - \tilde{\nu}^2 - i2\beta\tilde{k}} + i\tilde{\nu}. \tag{26}$$

Since a small inhomogeneity of the microparticle cloud is assumed, it must be $|\beta|\tilde{k} \ll q^2$. Then, for the real and imaginary parts of the complex frequency $\tilde{\omega} = \omega' + i\omega''$, we derive

$$\omega' \simeq \sqrt{q^2 - \tilde{\nu}^2} \tag{27}$$

and

$$\omega'' \simeq \tilde{\nu} - \frac{\beta\tilde{k}}{\sqrt{q^2 - \tilde{\nu}^2}}. \tag{28}$$

From (27), the phase velocity is

$$c_{\text{ph}} = c_d\frac{\omega'}{\tilde{k}} = c_d\sqrt{\alpha^2 + \frac{1-\tilde{\nu}^2}{\tilde{k}^2} + \frac{1}{\tilde{k}^2(\tilde{k}^2+1)}} \tag{29}$$

and the group velocity can be expressed as

$$c_{\text{gr}} = c_d\frac{d\omega'}{d\tilde{k}} = \frac{c_d^2}{c_{\text{ph}}}\left[\alpha^2 - \frac{1}{(\tilde{k}^2-1)^2}\right]. \tag{30}$$

Since $c_{\text{gr}}$ vanishes for the wave number $\tilde{k} = \tilde{k}_0 = \sqrt{1+\alpha^{-1}}$, the minimum frequency $\omega'_{\text{min}}$, for which the wave propagation is possible, is

$$\omega'_{\text{min}} = \sqrt{(1+\alpha)^2 - \tilde{\nu}^2} = \sqrt{\alpha^2\tilde{k}_0^4 - \tilde{\nu}^2}. \tag{31}$$

PLEASE CITE THIS ARTICLE AS DOI: 10.1063/5.0094038

AIP Publishing

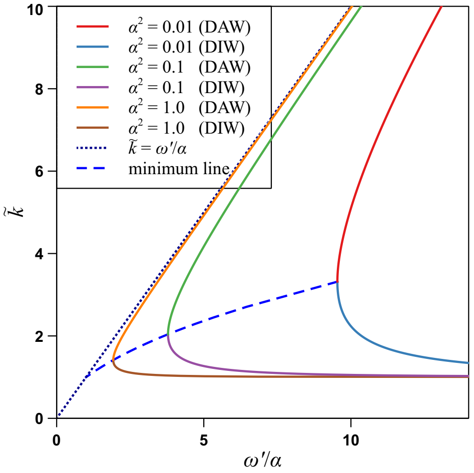

FIG. 1. Unified DIW–DAW dispersion relation (27) in dimensionless quantities for different $\alpha$; DIW and DAW branches are indicated by different colors (see legend). Dotted line shows the DAW high-frequency asymptote $\tilde{k} = \omega'/\alpha$ and dashed line that separates the DIW and DAW branches connects the points of $\omega'$ minima for different $\alpha$ and fixed $\tilde{\nu}^2 = 0.3$.

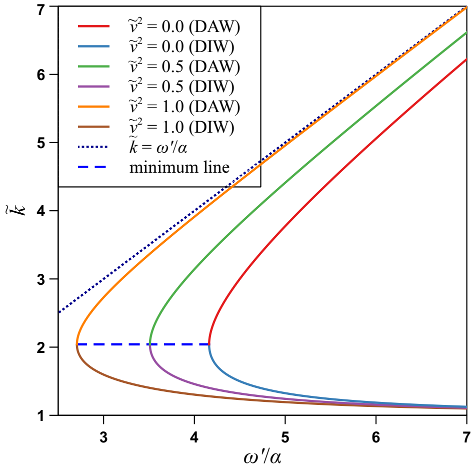

FIG. 2. The same as in Fig. 1. Dashed line connects the points of $\omega'$ minima for different $\tilde{\nu}$ (see legend) and fixed $\alpha^2 = 0.1$.

Therefore, one can conclude that there exists the cutoff frequency below which propagation of both DIW and DAW is impossible.

The effect of microparticle friction against neutrals leads to a notable decrease of the cutoff frequency. The unified dispersion relation is thus significantly modified by the inclusion of friction. It formally follows from (31) that $\omega'_{\min} = 0$ if $\tilde{\nu} = 1 + \alpha > 1$. However, for such a high friction, a rapid damping would prevent the wave propagation. Equation (31) means that the minimum frequency, at which propagation of both DIW and DAW is still possible, can be crudely estimated as $\omega_d$. It follows from (25) and (27) that for $\alpha^2 < 1$, $\tilde{k} > 1$, i.e., the lower bound for the wave number $k$ is $k_d$. For $\alpha^2 \geq 1$, lower $k$ can, in principle, be realized on the segment $0 \leq \tilde{k} \leq \sqrt{1-\alpha^{-2}}$ at $\tilde{\nu} = 0$. However, it is questionable if the condition $\alpha^2 \geq 1$ can be realized under experimental conditions.

Figure 1 shows the wave number vs. the real part of frequency in dimensionless quantities for different $\alpha$ and fixed $\tilde{\nu}$. Note that $\omega'$ (27) is independent of the instability coefficient $\beta$. As is seen, the unified dispersion relation has a hyperbolic form with the asymptotes $\tilde{k} = 1$ and $\tilde{k} = \omega'/\alpha$ at $\omega \to \infty$. The first asymptote corresponds to the DIW mode and the second one, to the DAW mode. The minimum line connects the points of minimum admissible $\omega'$ and the corresponding wave numbers $\tilde{k} = \tilde{k}_0$. The function $\tilde{k}_0(\omega'_{\min})$ decreases with the decreasing $\omega'_{\min}$ until it crosses the asymptote $\tilde{k} = \omega'/\alpha$ at $\omega'/\alpha = 1$ and $\tilde{k} = 1$ ($\tilde{\nu} = 0$) [see Eq. (31)]. For $\alpha > 1$, one more hyperbola emerges at $\omega'/\alpha < 1$ and $\tilde{k} < 1$ (see the discussion above), which passes through the point $\omega' = \tilde{k} = 0$. At $\alpha \to \infty$, this hyperbola coincides with the asymptote $\tilde{k} = \omega'/\alpha$, and the dispersion relation is degenerated to that of DAW, as it must. Note that $\omega'_{\min}/\alpha$ increases noticeably with the decrease in $\alpha$ (Fig. 1). Figure 2 illustrates the variation of dispersion relation with the reduced friction coefficient $\tilde{\nu}$ at fixed $\alpha$. As is seen, the dispersion relation preserves its form, and $\omega'_{\min}/\alpha$ decreases with the increase in $\tilde{\nu}$, the minimum line being parallel to abscissa. The dispersion relation for $\tilde{\nu} = 1$ is indeed a boundary of the wave propagation region arising from a significant wave damping due to the microparticle friction against neutrals.

## IV. COMPARATIVE ANALYSIS OF SPECIFIC WAVE MODES

Since the DIW mode corresponds to the extreme $\omega' \to \infty$ and $\tilde{k} \to 1$ (Fig. 1), it follows from (25) that in this extreme, $q \to \infty$. Then one can derive the following estimates from Eq. (27):

$$\tilde{k} \simeq 1 + \frac{1}{2}\left(\omega'^2 - \alpha^2 - 1 + \tilde{\nu}^2\right)^{-1} \tag{32}$$

and $\left(\tilde{k}^2 - 1\right)^{-2} \simeq \omega'^4$. As is seen from (32), the wave number decreases slowly down to unity with the increase in the real part of frequency. Thus, DIW is in fact a long-wave mode of non-acoustic type. If $k \simeq k_d$ then the phase velocity $c_{\text{ph}} \simeq \omega/k_d$ is proportional to the frequency. From (32), the group velocity $c_{\text{gr}} \simeq -c_d(\omega/\omega_d)^3 = -\omega^3/c_d^2 k_d^3$ is negative and depends on the frequency even more sensitively, and its absolute magnitude can be very high (Fig. 4). The DIW propagation is impossible in the region $k \leq k_d$ and $\omega < \omega_{\min}$.

AIP Publishing

Physics of Plasmas ACCEPTED MANUSCRIPT

This is the author's peer reviewed, accepted manuscript. However, the online version of record will be different from this version once it has been copyedited and typeset.

PLEASE CITE THIS ARTICLE AS DOI: 10.1063/5.0094038

The DAW mode is realized at $\omega' \to \infty$ and $\tilde{k} \to \infty$. In this extreme, from (25) and (27) one can readily derive the estimate

$$\omega' \simeq \sqrt{\alpha^2\tilde{k}^2 + 1 - \tilde{\nu}^2} \simeq \alpha\tilde{k} + \frac{1-\tilde{\nu}^2}{2\alpha\tilde{k}}, \qquad (33)$$

which corresponds to the acoustic-type waves at $k \to \infty$, i.e., DAW is a short-wave oscillation extreme. The term $(1-\tilde{\nu}^2)/2\alpha\tilde{k}$ in (33) is a correction to the classical linear dependence $\omega = c_a k$ arising from the effect of the microparticles on the dissociation rate. Due to this effect, every tangent to the dispersion relation curve in its short-wave branch does not pass through the origin of the coordinate system (Fig. 1). From (33), the DAW phase and group velocity are

$$c_{\text{ph}} \simeq c_a \sqrt{1 + \frac{1-\tilde{\nu}^2}{\alpha^2\tilde{k}^2}} \qquad (34)$$

and

$$c_{\text{gr}} \simeq \frac{\alpha^2 c_d \tilde{k}}{\omega'} = \frac{c_a}{\sqrt{1 + \frac{1-\tilde{\nu}^2}{\alpha^2\tilde{k}^2}}} = \frac{c_a^2}{c_{\text{ph}}}, \qquad (35)$$

respectively. Both of them include the corrections from the ionization kinetics and $c_{\text{gr}}$ is positive, as it must. From (35), we have $c_a = \sqrt{c_{\text{gr}} c_{\text{ph}}}$.

It is of interest to estimate the amplitude ratio $\left|Zn'_d/n'_e\right|$ for both wave modes. If we treat the wave solution $n'_e = Ce^{i(\omega t - kx)}$, $n'_d = Be^{i(\omega t - kx)}$, where $C$ and $B$ are constants, and set $\nu = A = 0$ for the sake of simplicity then we obtain from (19) and (23)

$$\frac{BZ}{C} = -\frac{H^2}{1+2H} \frac{c_d^2 k^2}{\omega^2 - c_a^2 k^2}. \qquad (36)$$

For the DIW mode, we have $k \simeq k_d$, $\omega \gg c_a k_d$, and $H^2(1+2H)^{-1} \sim 1$ at $H > 1$. Then at sufficiently high frequencies, $\left|Zn'_d/n'_e\right| \sim \omega_d^2/\omega^2 \ll 1$. Therefore, from (17) we have $n'_e \simeq n'_i$, which means that variations of the electron and ion fluxes almost coincide. Hence, the DIW oscillations must have no significant effect on the microparticle charge. This justifies the assumption $Z = $ const assumed for linearization of Eq. (5). In contrast, for the DAW mode we have from (33) $\omega^2 - c_a^2 k^2 \simeq \omega_d^2$ ($\tilde{\nu} = 0$), therefore, in this mode $\left|Zn'_d/n'_e\right| \sim k^2/k_d^2 \gg 1$. This means that for DAW, the oscillations of $n'_e$ are small and $n'_i \simeq Zn'_d$.

Equation (36) allows one to estimate the ratio $\eta$ of the first and second term on the right-hand side of the master equation (5). For small perturbations, this ratio is equal to the corresponding ratio of the first and second term on the right-hand side of the first Eq. (15):

$$\eta = -\alpha^2 \frac{1+2H}{H^2} \frac{\partial (Zn'_d)}{\partial x} \left(\frac{\partial n'_e}{\partial x}\right)^{-1}. \qquad (37)$$

For the wave solution and consequent amplitude ratio (36), (37) is transformed to

$$\eta = \frac{c_a^2 k^2}{\omega^2 - c_a^2 k^2}. \qquad (38)$$

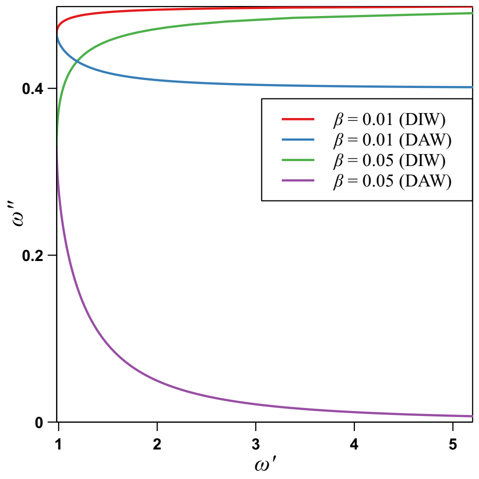

FIG. 3. Imaginary vs. real part of the complex frequency at the DIW and DAW branches (indicated by different colors) calculated by formulas (27) and (28) for different $\beta$ (see legend) at fixed $\alpha = 0.01$ and $\tilde{\nu} = 0.5$.

Hence, for the DIW mode, $\eta \simeq (\alpha\omega_d/\omega)^2 \ll 1$, i.e., the term including the electric field dominates over that taking into account the microparticle cloud compressibility while for the DAW mode, $\eta \simeq (\alpha k/k_d)^2 \gg 1$. Note that along the acoustic branch, the cloud compressibility dominates over the DIW electric field term if only $\alpha$ is not too small. Otherwise, the DIW correction to the acoustic dispersion relation (33) may not be small.

Now turn to the imaginary part of the frequency. From Eq. (28) for DIW, it follows that $\omega'' \simeq \tilde{\nu}$, i.e., the temporal change of the wave amplitude is defined solely by the dust particle friction against neutrals that results in the wave damping. In this case, the amplitude increment due to the instability development mechanism taken into account by the last term in Eq. (5) can obviously be ignored. In contrast, the imaginary part of the frequency for the DAW mode is $\omega'' \simeq \tilde{\nu} - \beta/\alpha$. Thus, in this mode, the self-excited microparticle oscillations emerge if $\omega'' < 0$, i.e., $\tilde{\nu} < \beta/\alpha$; otherwise, DAW must rapidly decay. The difference in the dependencies of DIW and DAW on the friction and instability coefficients is illustrated by Fig. 3 that presents the imaginary part of the frequency as a function of its real part at fixed $\alpha$ and $\tilde{\nu}$. This figure shows that at $\omega' > \omega'_{\min}$, the DIW and DAW dependencies are qualitatively different: for DIW, $\omega''$ is almost constant, and it is almost independent on $\beta$ while for DAW, the dependence of $\omega''$ on $\beta$ is very sharp. For this mode, $\omega''$ can be negative ($\beta = 0.05$ in Fig. 3 corresponds to the threshold of DAW self-excitation). It will be shown in Sec. V that such different behavior of wave damping in combination with the high phase velocity of DIW has a pronounced effect on the wave damping length, which proved to be much larger than

Physics of Plasmas

PLEASE CITE THIS ARTICLE AS DOI: 10.1063/5.0094038

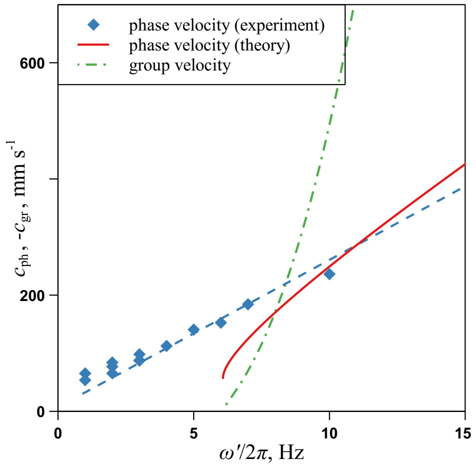

FIG. 4. Phase and group velocity of DIW $c_{\text{ph}}$ and $c_{\text{gr}}$, respectively, as functions of the frequency real part for the conditions of experiment[30] (see text). The results of $c_{\text{ph}}$ and $c_{\text{gr}}$ calculations by formulas (29), (30), and (27) are shown by solid and dashed-dotted line, respectively. Dots indicate the results of experiment[30] and dashed line shows extrapolation of these data to higher frequencies.

for DAW. This enables experimental observation of the excited DIW.

## V. DISCUSSION

In this Section, numerical estimates for the key parameters of above-discussed theory under typical experimental conditions are performed. To estimate the DIW parameters $k_d$ (21) and $\omega_d$ (22), it is sufficient to calculate $Rn_{d0}$. Since $Rn_{i0}$ is the recombination rate on a single particle, the flux of electrons on a particle can be approximated by the expression $\sqrt{8\pi} n_{e0} v_{Te} a^2 e^{-\Phi}$, where $v_{Te} = \sqrt{T_e/m_e}$. Therefore,

$$Rn_{d0} = \sqrt{8\pi}\frac{v_{Te} n_{d0} a^2}{1+H} e^{-\Phi}. \tag{39}$$

The ion diffusion coefficient required for calculation of the parameters $k_d$ and $\omega_d$ is estimated as $D = \sqrt{8/9\pi} v_{Ti}/n_a \sigma_{ia}$, where $v_{Ti} = (T_i/m_i)^{1/2}$ is the ion thermal velocity; $n_a = p_{\text{gas}}/T_a$, $p_{\text{gas}}$ and $T_a = T_i = 300$ K are the pressure and temperature of neutrals, respectively; and $\sigma_{ia} \simeq 2 \times 10^{-14}$ cm$^2$ is the ion–neutral collision cross-section.[37]

Under the conditions of experiment[30], one can adopt he following input parameters: $n_{i0} = 10^8$ cm$^{-3}$, $n_{d0} = 7 \times 10^4$ cm$^{-3}$, $Z = 10^3$ (i.e., $H = 2.4$), $2a = 3.38 \times 10^{-4}$ cm, $T_e = 3$ eV, the argon pressure $p_{\text{gas}} = 11.5$ Pa, and the resulting friction coefficient $\nu = 41.4$ Hz. Thus, we obtain and $\omega_d/2\pi = 6.27$ Hz, $\omega'_{\text{min}}/2\pi = 6.08$ Hz, $k_d = 2.02$ cm$^{-1}$, $c_d = 19.5$ cm s$^{-1}$, and $\tilde{\nu}^2 = 0.276$. With a typical value $c_a = 2.0$ cm s$^{-1}$, we have $\alpha^2 = 1.05 \times 10^{-3}$. To compare the dispersion relation (32) with that obtained from experiment (Fig. 10 in Ref. 30), one has to bear in mind that in this experiment, DIW was externally excited in a finite microparticle cloud whose length does not exceed two to three DIW wavelengths $2\pi/k_d$. At the same time, the theory proposed in this work implies the free wave propagation in an infinite cloud. Then, at the minimum (cutoff) frequency, the wave propagation must be transformed into the forced vibrations of a whole cloud analogous to the forced vibrations of an elastic body rather than to the wave propagation in an infinite medium. From this viewpoint, the cutoff frequency $\omega'_{\text{min}}/2\pi$ can be associated with a sharp drop of $k$ with the decreasing excitation frequency less than 3 Hz. Then, the characteristic wave vector $k_d$ should be juxtaposed with the experimental data at the excitation frequencies above 3 Hz. It is noteworthy that at the lower frequencies, experimental $k$ drops almost exactly to $2\pi/L$, where $L$ is the microparticle cloud length, and this was observed for both argon and neon. Note additionally that at the excitation frequencies above 3 Hz, the frequency dependence of $k$ may be dependent on the choice of the coordinate interval selected for the recovery of dispersion relation demonstrating both weakly increasing and decreasing trends, the drop of experimental $k$ in the vicinity of the cutoff frequency being more or less pronounced. Thus, from Fig. 10 in Ref. 30, one can conclude that the theory overestimates the cutoff frequency by two to three times while $k_d$ is in a good agreement with the experiment. Such a situation is a consequence of a weak dependence of $k_d$ on the complex plasma parameters and sensitivity of $\omega'_{\text{min}}$ to these parameters (see the discussion below). A quantitative mismatch for $\omega'_{\text{min}}$ may also arise from such factors as the above-mentioned finite length of the microparticle cloud, significant inhomogeneity of the latter in the direction of the discharge axis not taken into account in the theory, and the transverse oscillations mentioned in[30] and not allowed for in the proposed model. Another source of disagreement can be the ionization–recombination kinetics Eq. (11). Albeit the effective ionization coefficient rather than the real one is implied in this equation, the approximation of ionization by electron impact may be too crude for the discharge in argon. Additional source of errors can be neglect of the dependence of recombination term on the electron number density.

In spite of the cutoff frequency shift, proposed theory that includes no adjustable parameters can be compatible with experimental data. Figure 4 shows the phase velocity (29) calculated for the DIW mode and juxtaposed with the results of its experimental determination.[30] Since the slope of a curve that approximates the experimental dependence of $c_{\text{ph}}$ on the excitation frequency is almost constant, it is possible to extrapolate this dependence to the higher frequencies up to 15 Hz, where the microparticle oscillations were not resolved experimentally. One can see that at $\omega'/2\pi \geq 7$ Hz, the calculation results correlate with experimental data and their extrapolation. The slopes of the calculated and extrapolation curves are not much different. Note that correlation between the theory and experiment could be significantly improved if $\omega'_{\text{min}}$ was an adjustable parameter. The high phase velocities as compared to the typical DAW velocity, both calculated and experimen-

Physics of Plasmas ACCEPTED MANUSCRIPT
This is the author's peer reviewed, accepted manuscript. However, the online version of record will be different from this version once it has been copyedited and typeset.
PLEASE CITE THIS ARTICLE AS DOI: 10.1063/5.0094038

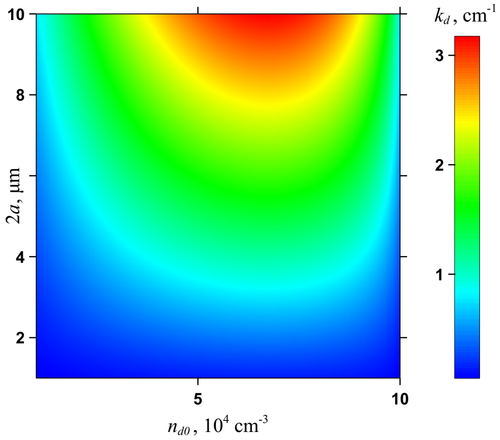

FIG. 5. Characteristic DIW wave number $k_d$ (21) as a function of the microparticle number density $n_{d0}$ and diameter $2a$ for $n_{i0} = 10^8$ cm$^{-3}$, $Z = 10^3$, $T_e = 3$ eV, and the argon pressure $p_{\mathrm{gas}} = 11.5$ Pa.

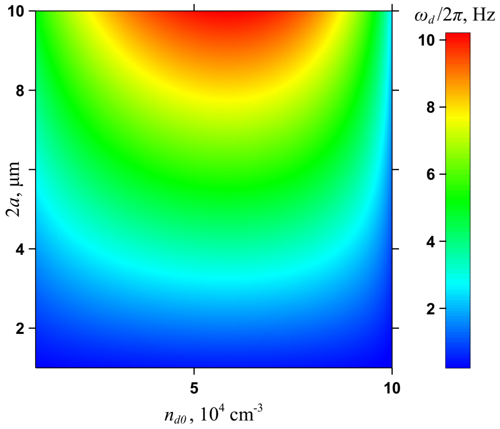

FIG. 6. Characteristic DIW frequency $\omega_d$ (22) as a function of the microparticle number density $n_{d0}$ and diameter $2a$ for $n_{i0} = 10^8$ cm$^{-3}$, $Z = 10^3$, $T_e = 3$ eV, and the argon pressure $p_{\mathrm{gas}} = 11.5$ Pa.

tal, are worth mentioning. The group velocity $c_{\mathrm{gr}}$ for the DIW mode (30) is even higher in absolute magnitude (Fig. 4). Note its negative sign that is characteristic of the ionization waves in the pure gas discharge.

Figures 5 and 6 illustrate the sensitivity of key parameters, $k_d$ and $\omega_d$, to the microparticle number density and diameter, other parameters being fixed. It is seen that at $2a < 8$ $\mu$m, both parameters depend on $n_{d0}$ rather weakly in the interval $n_{d0} = (7 \pm 2) \times 10^4$cm$^{-3}$. It is noteworthy, however, that in real complex plasma, all parameters are related. In any case, the variation range of $k_d$ is notably smaller than that of $\omega_d$, which means essentially weaker sensitivity of $\omega_d$ to the complex plasma parameters.

One more important parameter relevant for the wave propagation is the damping length. For both DIW and DAW modes, the latter can be estimated as $\delta l = c_{\mathrm{ph}}/\omega_d\omega''$. For the DIW mode at large frequences, $c_{\mathrm{ph}} \simeq \omega/k_d$, and from Eq. (28), $\omega_d\omega'' \simeq \nu/2$ (see discussion in Sec. IV). Therefore, $\delta l = 2\omega/\nu k_d \to \infty$ as $\omega \to \infty$. A typical damping length for $\omega = \omega_d$ is thus $\delta l = 2c_d/\nu$. For the estimates above ($c_d = 19.5$ cm s$^{-1}$ and $\nu = 41.4$ Hz), we arrive at the estimate $\delta l \simeq 1$ cm, which is on the same order of magnitude as the length of the camera field of view in the experiment.[30] Hence, due to a considerable scatter of data and the microparticle cloud inhomogeneity damping of the excited DIW can scarcely by detected. Since $\nu$ is proportional to $p_{\mathrm{gas}}$ and $c_d$ is independent of the gas pressure [Eq. (23)], $\delta l$ is inversely proportional to $p_{\mathrm{gas}}$. This means that the pressure $p_{\mathrm{gas}} \sim 20$ Pa is the maximum one, for which DIW are observable at $\omega \sim \omega_d$.

Instead, for the DAW mode, $c_{\mathrm{ph}} \simeq c_a$ and according to Eq. (28), $\omega_d\omega'' \simeq \nu/2 - \beta\omega_d/\alpha$. In the case that the instability coefficient $\beta$ vanishes, the damping length $\delta l \simeq 2c_a/\nu$ becomes very short. For $c_a = 2.0$ cm s$^{-1}$, it amounts to $\delta l \simeq 0.1$ cm, which is much smaller than the microparticle cloud length and even smaller than the DAW wavelength, which is larger than at least 0.2 cm. However, $\delta l = 2\alpha c_a/(\alpha\nu - 2\beta\omega_d) \to \infty$ as $\beta \to \alpha\nu/2\omega_d$, which is illustrated by Fig. 3. Thus, one can conclude that DIW can be externally excited but DIW self-excitation is impossible. Instead, under proper conditions, DAW can be self-excited but it is difficult to observe the externally excited DAW.

## VI. CONCLUSION

In conclusion, a theoretical interpretation of DIW recently observed experimentally on PK-4 setup on board the ISS is proposed in this paper. The progressing waves were formed in the elongated cloud of microparticles formed in the low-pressure DC argon discharge. It was demonstrated that DIW emerge due to the charge separation in plasma resulting from the inhomogeneity of microparticle spatial distribution and the consequent inhomogeneity of recombination rate. The momentum equation for the "fluid" of microparticles also accounts for the proper compressibility of the microparticle cloud, friction of the microparticles against neutrals, and the interaction between microparticles and streaming ions that may lead to emergence of the self-excited oscillations.

We solve the linearized master equations to obtain the dispersion relation $\omega(k)$. Notably, this dispersion relation is a junction of the DIW and DAW branches. Its significant property is the existence of some cutoff frequency, below which the wave propagation is impossible, and which is a point of mode junction. In the extreme of high frequencies, the low wave number $k_d$ that is almost independent of the frequency is characteristic of the DIW branch while the high wave numbers proportional to the frequency can be found along the DAW branch. Since the DIW phase velocity scale $c_d$ is typically

Physics of Plasmas ACCEPTED MANUSCRIPT

This is the author's peer reviewed, accepted manuscript. However, the online version of record will be different from this version once it has been copyedited and typeset.

PLEASE CITE THIS ARTICLE AS DOI: 10.1063/5.0094038

much higher than that for the DAW ($c_d \gg c_a$), the DIW phase velocity can be very high. At the same time, the ionization correction to the DAW dispersion relation leads to the deviation from the direct proportionality $\omega = c_a k$. The DIW group velocity is negative, which is a notable peculiarity of this wave mode.

We have shown that the wave damping is quite different for DIW and DAW. For DIW, damping is almost independent of the instability coefficient, and, consequently, self-excitation of DIW is impossible. However, due to the high phase velocity the DIW damping length can be comparable with the length of the microparticle cloud even in the case that the inverse time of the microparticle deceleration is comparable to the real part of the frequency. In contrast, for DAW the self-excited waves can be excited under appropriate conditions. At the same time, in the absence of instability the DAW damping length is positively too short to observe DAW in the experiment.

The estimates performed for the conditions of experiment[30] lead to the characteristic wave number that is in a good agreement with the experiment and to the characteristic frequency two to three times higher than the experimental one. Possible reasons for such mismatch are finiteness of the microparticle cloud length that is on the same order of magnitude as the DIW wavelength, a significant inhomogeneity of the microparticle number density in the cloud, neglect of the excited cloud radial (transverse) oscillations noted in Ref. 30, inaccuracy in the assumption of the ionization by electron impact, which is not the main channel of argon ionization, and disregarded dependence of the recombination coefficient on the electron number density. It is worth mentioning that, in spite of some discrepancy in the minimum frequency, the proposed theory matches the experimental dependence of the DIW phase velocity on the frequency.

Apparently, DIW can be excited under special conditions including a sufficient length of the microparticle cloud much larger than the wavelength and a strong effect of the microparticles on both the charge balance and recombination rate, which seems to encounter closer to the threshold of the discharge extinction caused by the presence of microparticles. The latter situation implies the large Havnes parameters of complex plasma. The lack of sufficiently accurate experimental data concerning DIW complicates both the comparison between theory and experiment and improvement in understanding of this phenomenon. Hopefully, future experiments will clarify the dispersion relation behavior in the regions of cutoff frequency and high frequencies. As for the theory, interaction between the incident DIW and the finite-geometry cloud of microparticles whose length is of the same order of magnitude as the wavelength is a separate problem to be addressed in future. However, the solution of this problem can be based on treatment of the problem of DIW propagation in an infinite medium.

## ACKNOWLEDGMENTS

This research is supported by the Russian Science Foundation Grant No. 20-12-00365.

## DATA AVAILABILITY

The data that supports the findings of this study are available within the article.

[1] V. E. Fortov and G. E. Morfill, eds., *Complex and Dusty Plasmas: From Laboratory to Space*, Series in Plasma Physics (CRC Press, Boca Raton, FL, 2010).

[2] C. K. Goertz, Rev. Geophys. **27**, 271 (1989).

[3] V. N. Tsytovich, A. V. Ivlev, A. Burkert, and G. E. Morfill, Astrophys. J. **780**, 131 (2014).

[4] J. H. Chu and I. Lin, Phys. Rev. Lett. **72**, 4009 (1994).

[5] H. Thomas, G. E. Morfill, V. Demmel, J. Goree, B. Feuerbacher, and D. Möhlmann, Phys. Rev. Lett. **73**, 652 (1994).

[6] Y. Hayashi and S. Tashibana, Jpn. J. Appl. Phys. **33**, L804 (1994).

[7] G. E. Morfill, H. M. Thomas, U. Konopka, H. Rothermel, M. Zuzic, A. Ivlev, and J. Goree, Phys. Rev. Lett. **83**, 1598 (1999).

[8] M. Schwabe, S. K. Zhdanov, H. M. Thomas, A. V. Ivlev, M. Rubin-Zuzic, G. E. Morfill, V. I. Molotkov, A. M. Lipaev, V. E. Fortov, and T. Reiter, New J. Phys. **10**, 033037 (2008).

[9] S. A. Khrapak, B. A. Klumov, P. Huber, V. I. Molotkov, A. M. Lipaev, V. N. Naumkin, H. M. Thomas, A. V. Ivlev, G. E. Morfill, O. F. Petrov, V. E. Fortov, Yu. Malentschenko, and S. Volkov, Phys. Rev. Lett. **106**, 205001 (2011).

[10] H. M. Thomas, G. E. Morfill, V. E. Fortov, A. V. Ivlev, V. I. Molotkov, A. M. Lipaev, T. Hagl, H. Rothermel, S. A. Khrapak, R. K. Suetterlin, M. Rubin-Zuzic, O. F. Petrov, V. I. Tokarev, and S. K. Krikalev, New J. Phys. **10**, 033036 (2008).

[11] M. Schwabe, K. Jiang, S. Zhdanov, T. Hagl, P. Huber, A. V. Ivlev, A. M. Lipaev, V. I. Molotkov, V. N. Naumkin, K. R. Sütterlin, H. M. Thomas, V. E. Fortov, G. E. Morfill, A. Skvortsov, and S. Volkov, Europhys. Lett. **96**, 55001 (2011).

[12] N. N. Rao, P. K. Shukla, and M. Y. Yu, Planet. Space Sci. **38**, 543 (1990).

[13] N. D'Angelo, J. Phys. D: Appl. Phys. **28**, 1009 (1995).

[14] R. L. Merlino, J. Plasma Phys. **80**, 773 (2014).

[15] A. Barkan, R. L. Merlino, and N. D'Angelo, Phys. Plasmas **2**, 3563 (1995).

[16] C. Thompson, A. Barkan, N. DAngelo, and R. L. Merlino, Phys. Plasmas **4**, 2331 (1997).

[17] V. E. Fortov, A. G. Khrapak, S. A. Khrapak, V. I. Molotkov, A. P. Nefedov, O. F. Petrov, and V. M. Torchinsky, Phys. Plasmas **7**, 1374 (2000).

[18] F. Melandso, Phys. Plasmas **3**, 3890 (1996).

[19] H. Ohta and S. Hamaguchi, Phys. Rev. Lett. **84**, 6026 (2000).

[20] M. Rosenberg and G. Kalman, Phys. Rev. E **56**, 7166 (1997).

[21] G. Kalman, M. Rosenberg, and H. E. DeWitt, Phys. Rev. Lett. **84**, 6030 (2000).

[22] B. M. Alotaibi, Rev. Geophys. **96**, 125273 (2021).

[23] A. E. Dubinov and I. N. Kitayev, Planet. Space Sci. **195**, 105142 (2021).

[24] P. Bajaj, S. Khrapak, V. Yaroshenko, and M. Schwabe, Phys. Rev. E **105**, 025202 (2022).

[25] P. K. Shukla and V. P. Silin, Phys. Scr. **45**, 508 (1992).

[26] S. Vladimirov, K. Ostrikov, and M. Yu, Phys. Rev. E **60**, 3257 (1999).

[27] P. Shukla and H. Rahman, Planet. Space Sci. **46**, 541 (1998).

[28] P. Shukla, M. Yu, and R. Bharuthram, J. Geophys. Res. Space Phys. **96**, 21343 (1991).

[29] M. Y. Pustylnik, M. A. Fink, V. Nosenko, T. Antonova, T. Hagl, H. M. Thomas, A. V. Zobnin, A. M. Lipaev, A. D. Usachev, V. I. Molotkov, O. F. Petrov, V. E. Fortov, C. Rau, C. Deysenroth, S. Albrecht, M. Kretschmer, M. H. Thoma, G. E. Morfill, R. Seurig, A. Stettner, V. A. Alyamovskaya, A. Orr, E. Kufner, E. G. Lavrenko, G. I. Padalka, E. O. Serova, A. M. Samokutyayev, and S. Christoforetti, Rev. Sci. Instrum. **87**, 093505 (2016).

[30] V. N. Naumkin, D. I. Zhukhovitskii, A. M. Lipaev, A. V. Zobnin, A. D. Usachev, O. F. Petrov, H. M. Thomas, M. H. Thoma, O. I. Skripochka, and A. A. Ivanishin, Phys. Plasmas **28**, 103704 (2021).

[31] P. Hartmann, M. Rosenberg, Z. Juhasz, L. S. Matthews, D. L. Sanford, K. Vermillion, J. Carmona-Reyes, and T. W. Hyde, Plasma Sources Sci. Technol. **29**, 115014 (2020).

[32] V. Tsytovich and K. Watanabe, Contrib. to Plasma Phys. **43**, 51 (2003).

[33] P. Shukla, L. Stenflo, and G. Morfill, IEEE Trans. Plasma Sci. **31**, 119 (2003).

Physics of Plasmas ACCEPTED MANUSCRIPT
This is the author's peer reviewed, accepted manuscript. However, the online version of record will be different from this version once it has been copyedited and typeset.
PLEASE CITE THIS ARTICLE AS DOI: 10.1063/5.0094038
AIP Publishing

[34] D. I. Zhukhovitskii, Phys. Plasmas **28**, 073701 (2021).
[35] D. I. Zhukhovitskii, Phys. Plasmas **26**, 063702 (2019).
[36] P. Epstein, Phys. Rev. **23**, 710 (1924).
[37] S. A. Khrapak, B. A. Klumov, P. Huber, V. I. Molotkov, A. M. Lipaev, V. N. Naumkin, A. V. Ivlev, H. M. Thomas, M. Schwabe, G. E. Morfill, O. F. Petrov, V. E. Fortov, Y. Malentschenko, and S. Volkov, Phys. Rev. E **85**, 066407 (2012).

AIP Publishing

Physics of Plasmas

ACCEPTED MANUSCRIPT

This is the author's peer reviewed, accepted manuscript. However, the online version of record will be different from this version once it has been copyedited and typeset.

PLEASE CITE THIS ARTICLE AS DOI: 10.1063/5.0094038

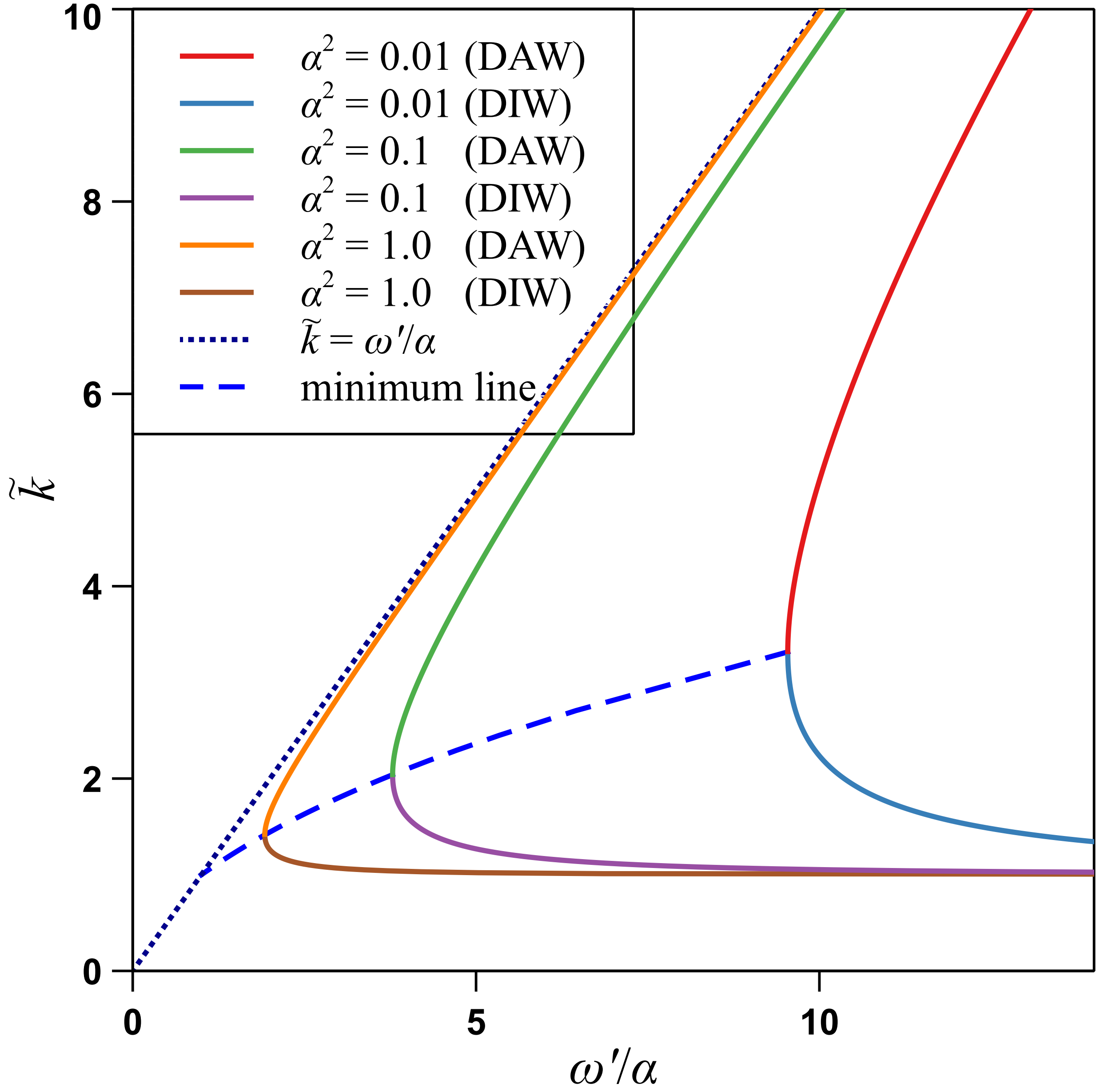

Physics of Plasmas ACCEPTED MANUSCRIPT

This is the author's peer reviewed, accepted manuscript. However, the online version of record will be different from this version once it has been copyedited and typeset.

PLEASE CITE THIS ARTICLE AS DOI: 10.1063/5.0094038

AIP Publishing

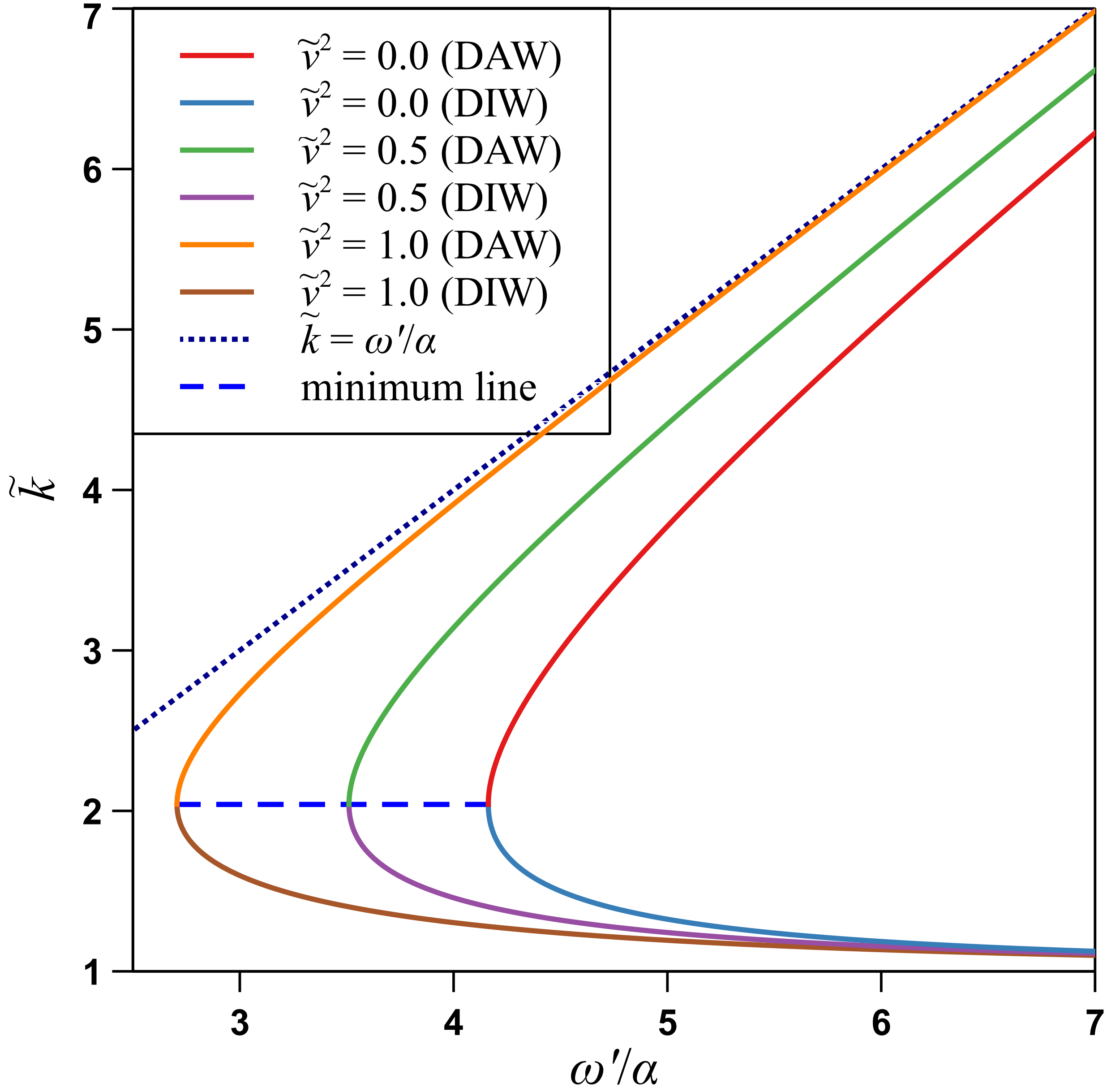

AIP Publishing
Physics of Plasmas
ACCEPTED MANUSCRIPT
This is the author's peer reviewed, accepted manuscript. However, the online version of record will be different from this version once it has been copyedited and typeset.
PLEASE CITE THIS ARTICLE AS DOI: 10.1063/5.0094038

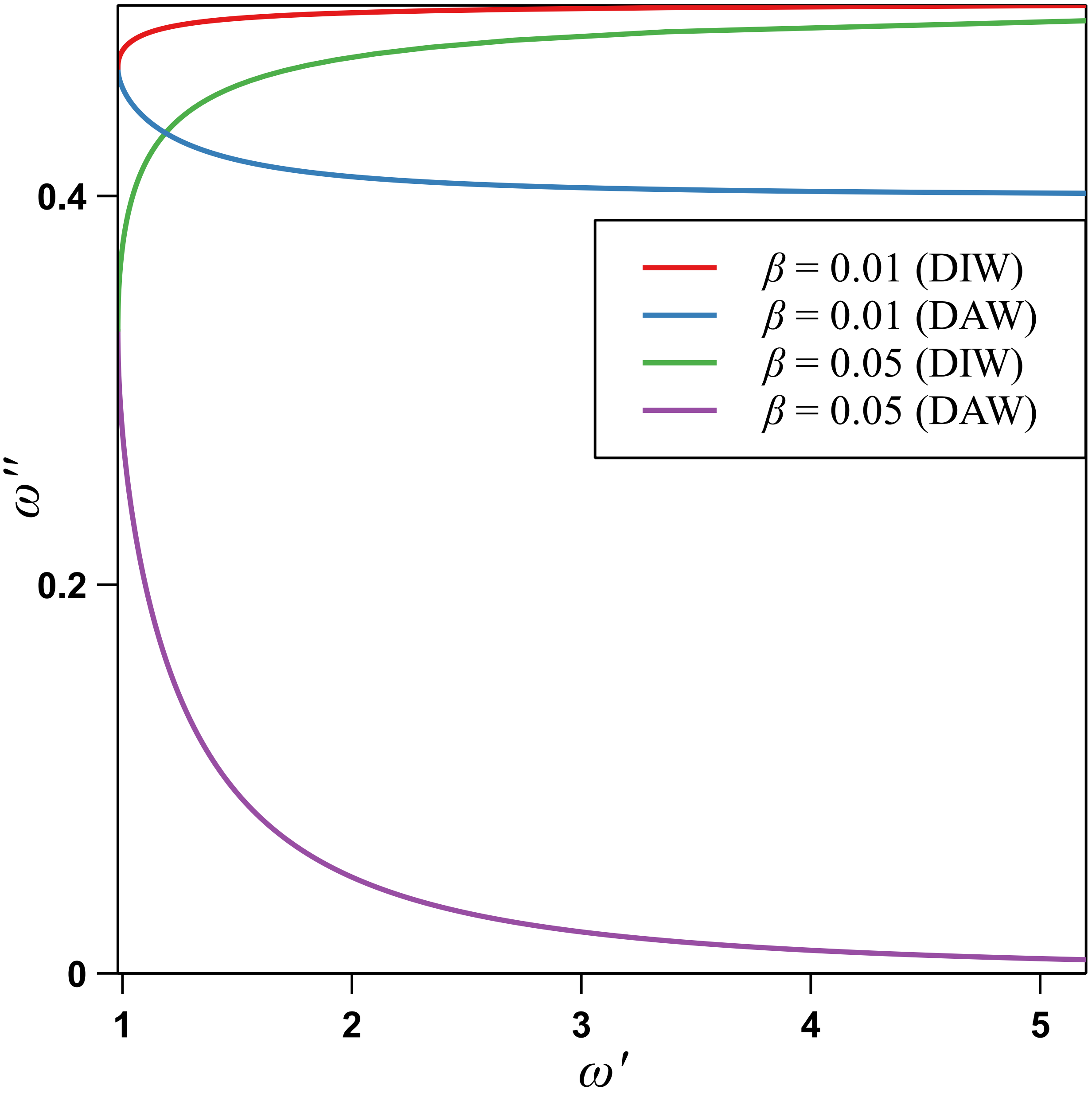

Physics of Plasmas ACCEPTED MANUSCRIPT

AIP Publishing

This is the author's peer reviewed, accepted manuscript. However, the online version of record will be different from this version once it has been copyedited and typeset.

PLEASE CITE THIS ARTICLE AS DOI: 10.1063/5.0094038

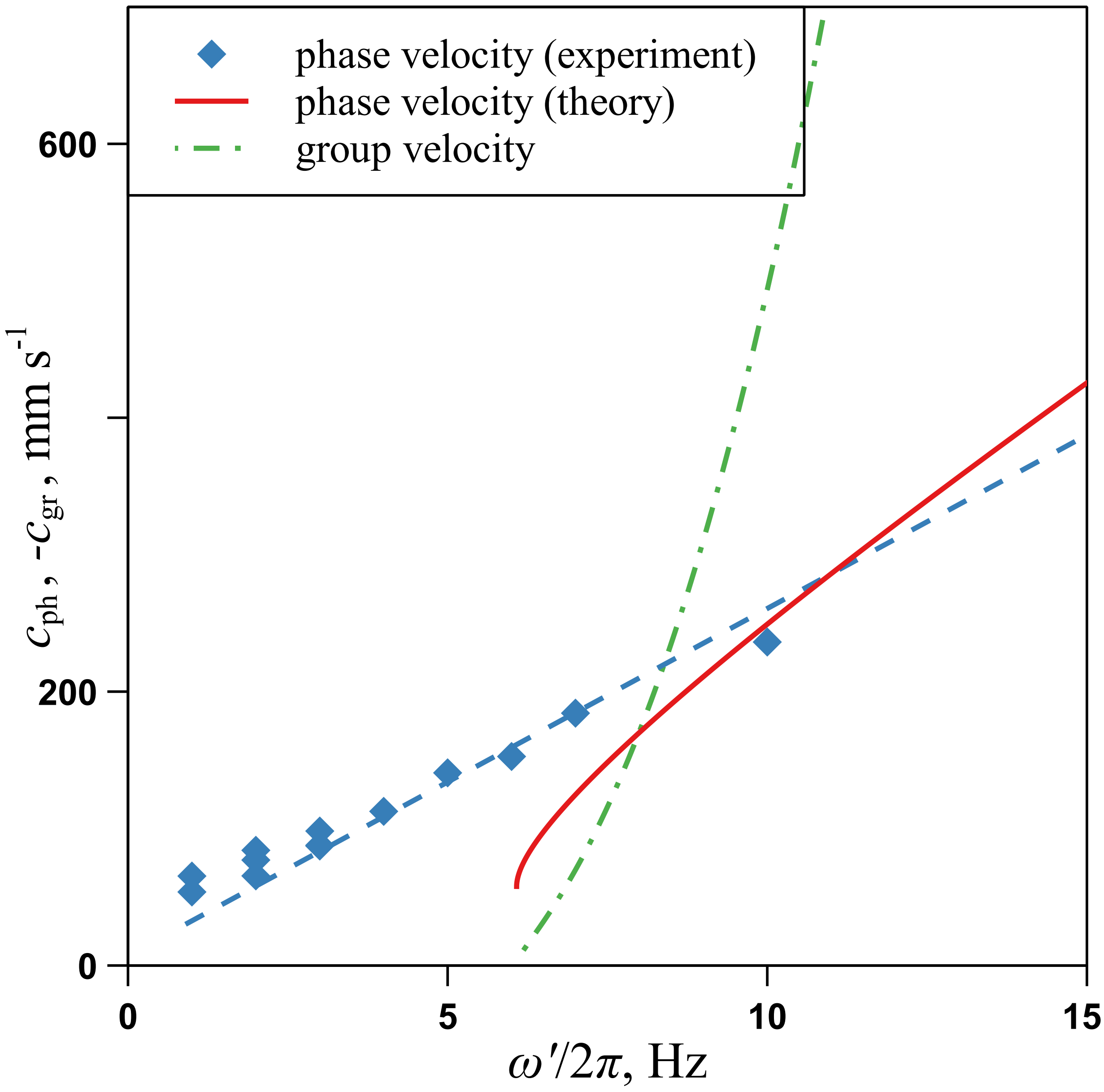

Physics of Plasmas ACCEPTED MANUSCRIPT

This is the author's peer reviewed, accepted manuscript. However, the online version of record will be different from this version once it has been copyedited and typeset.

PLEASE CITE THIS ARTICLE AS DOI: 10.1063/5.0094038

AIP Publishing

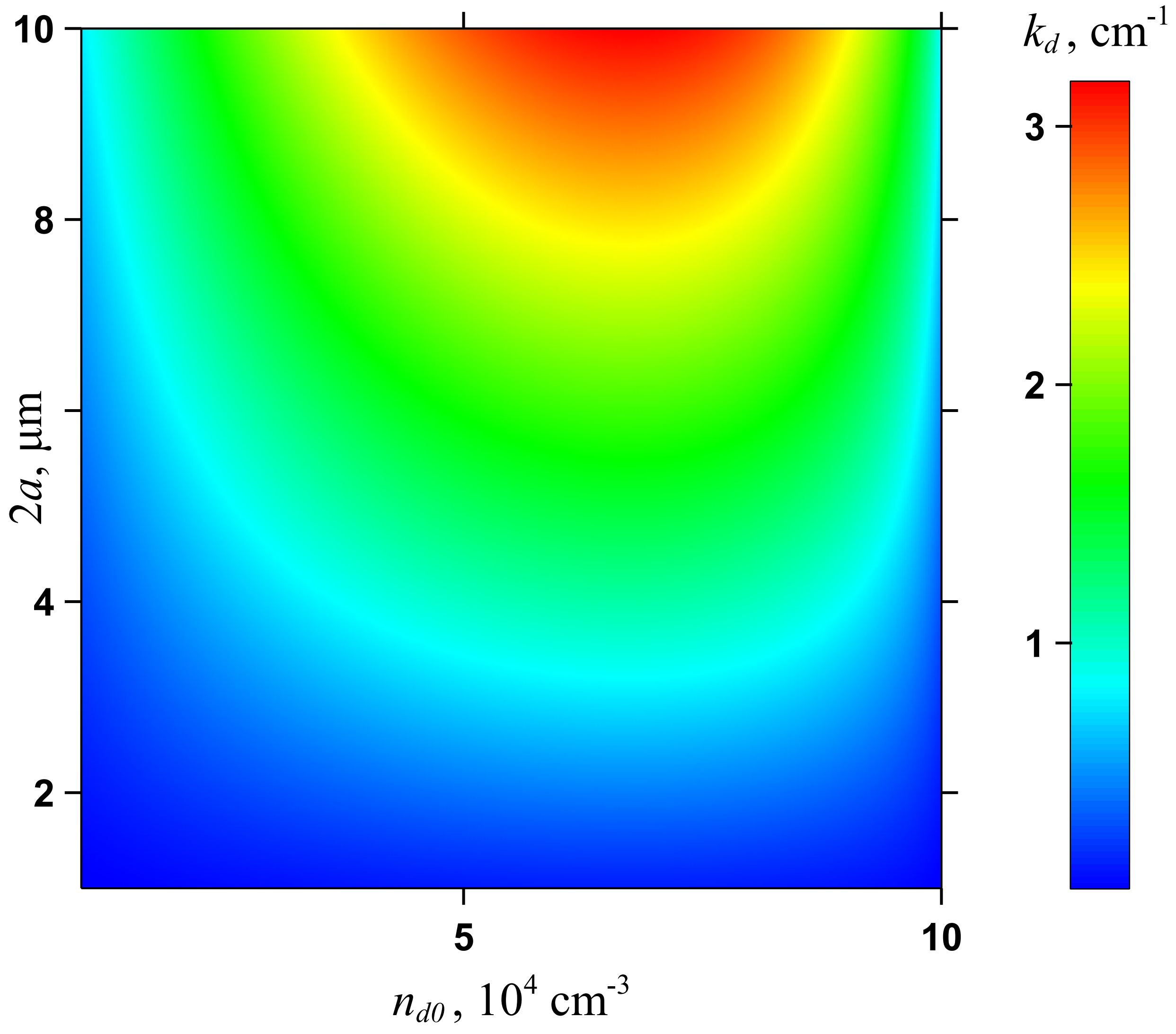

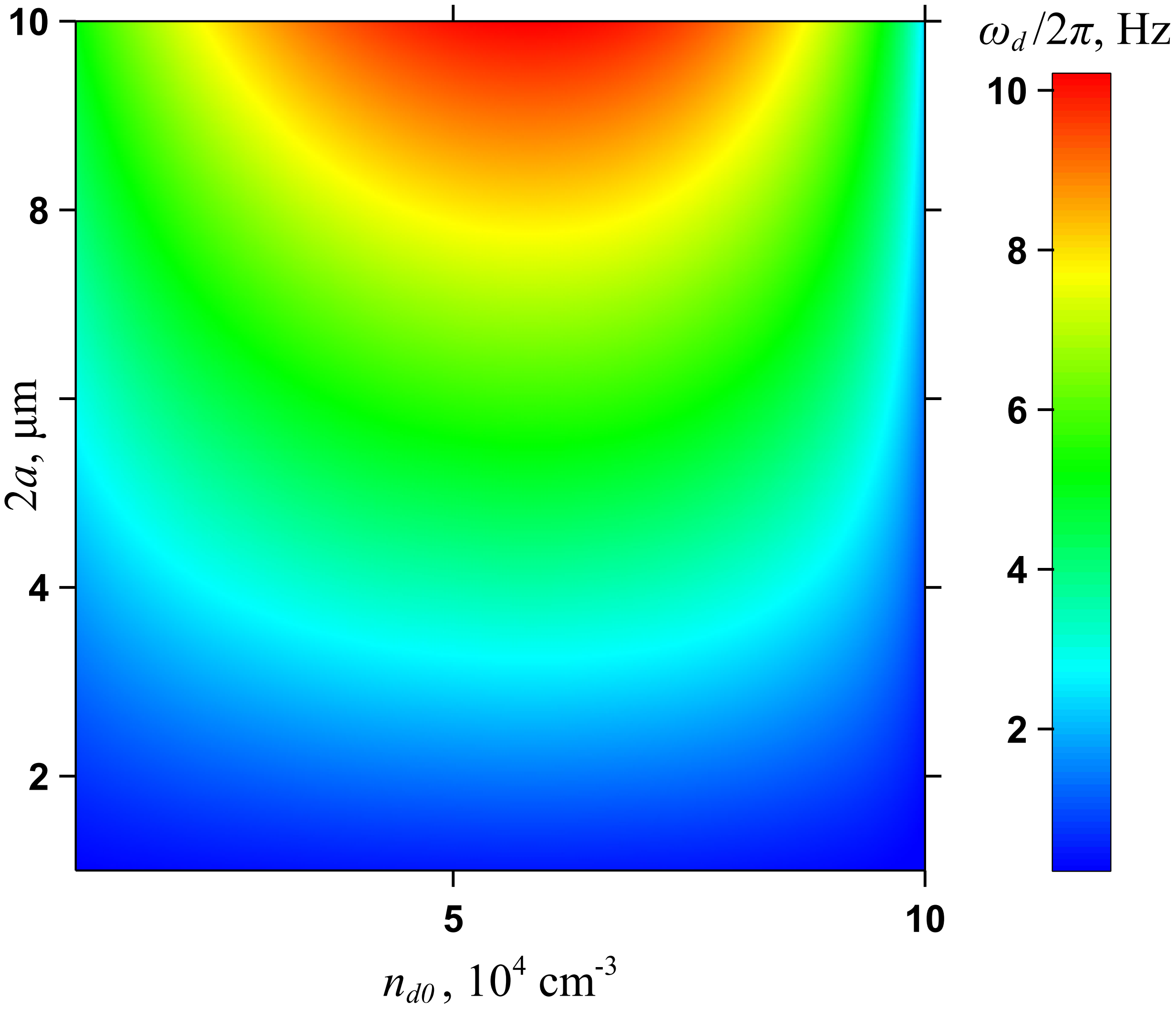ACCEPTED MANUSCRIPT
Physics of Plasmas
This is the author's peer reviewed, accepted manuscript. However, the online version of record will be different from this version once it has been copyedited and typeset.
PLEASE CITE THIS ARTICLE AS DOI: 10.1063/5.0094038
AIP Publishing